Supplementary Materials

Invader LNA – Efficient Targeting of Short Double Stranded DNA

Sujay P. Sau,[a] T. Santhosh Kumar[b] and Patrick J. Hrdlicka[a]*

a Department of Chemistry, University of Idaho, Moscow, ID 83844-2343, USA

b Nucleic Acid Center, Department of Physics and Chemistry, University of Southern Denmark, DK-5230 Odense M, Denmark
Corresponding author (PJH); Fax: (+1) 208 885 6173, E-mail: hrdlicka@uidaho.edu

Table S1. MALDI-MS of 2'-*N*-(pyren-1-yl)methyl-2'-amino-α-L-LNA **ON3**-**ON16**.[a]

	ON sequence	Experimental *m/z* $[M-H]^-$	Calculated *m/z* $[M-H]^-$
ON3	5'-d(GG**X** ATA TAT AGG C)	4255	4255
ON4	5'-d(GGT A**X**A TAT AGG C)	4251	4255
ON5	5'-d(GGT ATA **X**AT AGG C)	4252	4255
ON6	5'-d(GGT ATA TA**X** AGG C)	4252	4255
ON7	3'-d(CCA **X**AT ATA TCC G)	4135	4135
ON8	3'-d(CCA TA**X** ATA TCC G)	4132	4135
ON9	3'-d(CCA TAT A**X**A TCC G)	4132	4135
ON10	3'-d(CCA TAT ATA **X**CC G)	4132	4135
ON11	5'-d(GG**X** A**X**A TAT AGG C)	4493	4496
ON12	5'-d(GG**X** ATA **X**AT AGG C)	4496	4496
ON13	5'-d(GG**X** ATA TA**X** AGG C)	4496	4496
ON14	3'-d(CCA **X**A**X** ATA TCC G)	4377	4376
ON15	3'-d(CCA **X**AT A**X**A TCC G)	4375	4376
ON16	3'-d(CCA **X**AT ATA **X**CC G)	4375	4376

[a] For protocols of preparation and purification of 2'-*N*-(pyren-1-yl)methyl-2'-amino-α-L-LNA see ref S1. For the structure of 2'-*N*-(pyren-1-yl)methyl-2'-amino-α-L-LNA monomer **X**, see Fig. 1.

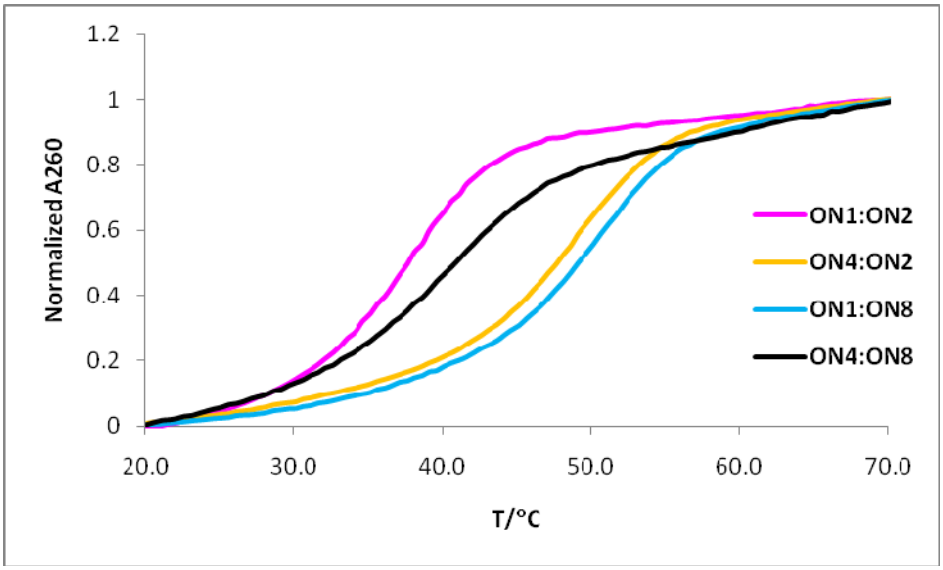

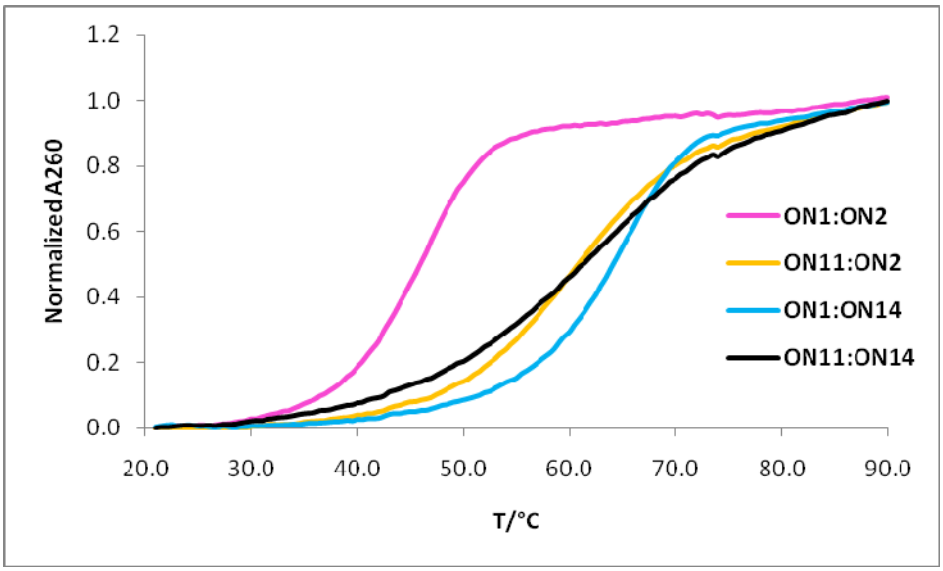

Figure S1. Representative thermal denaturation profiles. Upper panel: reference DNA duplex **ON1**:**ON2**, Invader LNA probe **ON4**:**ON8** and duplexes between 2'-*N*-(pyren-1-yl)methyl-2'-amino-α-L-LNA and complementary DNA **ON4**:**ON2** and **ON1**:**ON8** in medium salt conditions; Lower panel: DNA duplex **ON1**:**ON2**, Invader LNA probe **ON11**:**ON14** and duplexes between 2'-*N*-(pyren-1-yl)methyl-2'-amino-α-L-LNA and complementary DNA **ON11**:**ON2** and **ON1**:**ON14** in high salt conditions.

Table S2. Hybridization data for **ON3**-**ON16** vs complementary DNA at different ionic strengths.[a]

				T_m [ΔT_m] (ºC)			ΔG^{293} [$\Delta\Delta G^{293}$] (kJ/mol)		
Entry	ON	Duplex	**[Na^+] =**	10 mM	110 mM	710 mM	10 mM	110 mM	710 mM
1	**ON1**	5′-d(GGT ATA TAT AGG C)		18.5	37.5	45.5	-34	-57	-68
	ON2	3′-d(CCA TAT ATA TCC G)							
2	**ON3**	5′-d(GG**X** ATA TAT AGG C)		25.0	44.5	51.0	nd	-60	-67
	ON2	3′-d(CCA TAT ATA TCC G)		[+6.5]	[+7.0]	[+5.5]		[-3]	[+1]
3	**ON4**	5′-d(GGT A**X**A TAT AGG C)		29.5	47.5	55.5	-49	-66	-77
	ON2	3′-d(CCA TAT ATA TCC G)		[+11.0]	[+10.0]	[+10.0]	[-15]	[-9]	[-9]
4	**ON5**	5′-d(GGT ATA **X**AT AGG C)		30.5	49.0	56.0	-49	-69	-76
	ON2	3′-d(CCA TAT ATA TCC G)		[+12.0]	[+11.5]	[+10.5]	[-15]	[-12]	[-8]
5	**ON6**	5′-d(GGT ATA TA**X** AGG C)		28.5	47.0	54.5	-46	-66	-74
	ON2	3′-d(CCA TAT ATA TCC G)		[+10.0]	[+9.5]	[+9.0]	[-12]	[-9]	[-6]
6	**ON1**	5′-d(GGT ATA TAT AGG C)		29.7	48.5	56.0[b]	-46	-71	-77
	ON7	3′-d(CCA **X**AT ATA TCC G)		[+11.0]	[+11.0]	[+10.5]	[-12]	[-14]	[-9]
7	**ON1**	5′-d(GGT ATA TAT AGG C)		30.0	48.5	56.0	-47	-70	-78
	ON8	3′-d(CCA TA**X** ATA TCC G)		[+11.5]	[+11.0]	[+10.5]	[-13]	[-13]	[-10]
8	**ON1**	5′-d(GGT ATA TAT AGG C)		30.5	48.0	55.5	-50	-70	-76
	ON9	3′-d(CCA TAT A**X**A TCC G)		[+12.0]	[+10.5]	[+10.0]	[-16]	[-13]	[-8]
9	**ON1**	5′-d(GGT ATA TAT AGG C)		29.0	47.0	54.5	-48	-67	-74
	ON10	3′-d(CCA TAT ATA **X**CC G)		[+10.5]	[+9.5]	[+9.0]	[-14]	[-10]	[-6]
10	**ON11**	5′-d(GG**X** A**X**A TAT AGG C)		34.5	53.5	59.0	-57	-66	-71
	ON2	3′-d(CCA TAT ATA TCC G)		[+16.0]	[+16.0]	[+13.5]	[-23]	[-9]	[-3]
11	**ON12**	5′-d(GG**X** ATA **X**AT AGG C)		40.5	57.5	63.5	-62	-74	-75
	ON2	3′-d(CCA TAT ATA TCC G)		[+22.0]	[+20.0]	[+18.0]	[-28]	[-17]	[-7]
12	**ON13**	5′-d(GG**X** ATA TA**X** AGG C)		38.5	56.5	62.0	-60	-80	-77
	ON2	3′-d(CCA TAT ATA TCC G)		[+20.0]	[+19.0]	[+16.5]	[-26]	[-23]	[-9]
13	**ON1**	5′-d(GGT ATA TAT AGG C)		39.5	57.5	63.5	-61	-79	-84
	ON14	3′-d(CCA **X**A**X** ATA TCC G)		[+21.0]	[+20.0]	[+18.0]	[-27]	[-22]	[-16]
14	**ON1**	5′-d(GGT ATA TAT AGG C)		42.5	61.0	66.5	-67	-86	-87
	ON15	3′-d(CCA **X**AT A**X**A TCC G)		[+24.0]	[+23.5]	[+21.0]	[-33]	[-29]	[-19]
15	**ON1**	5′-d(GGT ATA TAT AGG C)		41.5	59.0	65.0	-63	-83	-88
	ON16	3′-d(CCA **X**AT ATA **X**CC G)		[+23.0]	[+21.5]	[+19.5]	[-29]	[-26]	[-20]

[a] T_m-values (ΔT_m = change in T_m-value relative to **ON1**:**ON2**) and Gibbs free energy of duplex formation at 293 K, ΔG^{293}, determined by baseline fitting of the optical melting curve (A_{260} vs T) recorded in low, medium or high salt buffer using 1.0 uM of each strands. All buffers are pH 7.0 (adjusted with NaH_2PO_4/Na_2HPO_4) and contain [Na^+] = 10/110/710 mM and [Cl^-] = 0/100/700 mM, respectively, for low/medium/high salt buffers. Values listed on a minimum of two measurements. $\Delta\Delta G^{293}$ = difference in Gibbs free energy of duplex formation relative to reference duplex **ON1**:**ON2**. For structure of monomer **X**, see Fig. 1. nd = not determined; [b] Based on single measurement only.

Table S3. Enthalpy and entropy of formation for duplexes between **ON3**-**ON16** and complementary DNA at different ionic strengths.[a]

				Δ*H* [ΔΔ*H*] (kJ/mol)			(T^{293}Δ*S*) [Δ(T^{293}Δ*S*)] (kJ/mol)		
Entry	ON	Duplex	**[Na^+] =**	10 mM	110 mM	710 mM	10 mM	110 mM	710 mM
	ON1	5′-d(GGT ATA TAT AGG C)		-419	-382	-403	-385	-325	-336
1									
	ON2	3′-d(CCA TAT ATA TCC G)							
	ON3	5′-d(GG**X** ATA TAT AGG C)		nd	-316	-331	nd	-256	-264
2									
	ON2	3′-d(CCA TAT ATA TCC G)			[+66]	[+72]		[+69]	[+72]
	ON4	5′-d(GGT A**X**A TAT AGG C)		-418	-356	-388	-370	-290	-311
3									
	ON2	3′-d(CCA TAT ATA TCC G)		[+1]	[+26]	[+15]	[+15]	[+35]	[+25]
	ON5	5′-d(GGT ATA **X**AT AGG C)		-387	-380	-371	-338	-311	-296
4									
	ON2	3′-d(CCA TAT ATA TCC G)		[+32]	[+2]	[+32]	[+47]	[+14]	[+40]
	ON6	5′-d(GGT ATA TA**X** AGG C)		-367	-358	-366	-321	-293	-293
5									
	ON2	3′-d(CCA TAT ATA TCC G)		[+52]	[+24]	[+37]	[+64]	[+32]	[+43]
	ON1	5′-d(GGT ATA TAT AGG C)		-409	-409	-381[b]	-363	-338	-304
6									
	ON7	3′-d(CCA **X**AT ATA TCC G)		[+10]	[-27]	[+22]	[+22]	[-13]	[+32]
	ON1	5′-d(GGT ATA TAT AGG C)		-359	-383	-389	-312	-314	-311
7									
	ON8	3′-d(CCA TA**X** ATA TCC G)		[+60]	[-1]	[+14]	[+73]	[+11]	[+25]
	ON1	5′-d(GGT ATA TAT AGG C)		-407	-390	-379	-357	-320	-302
8									
	ON9	3′-d(CCA TAT A**X**A TCC G)		[+12]	[-8]	[+24]	[+28]	[+5]	[+34]
	ON1	5′-d(GGT ATA TAT AGG C)		-430	-392	-371	-381	-325	-297
9									
	ON10	3′-d(CCA TAT ATA **X**CC G)		[-11]	[-10]	[+32]	[+4]	[0]	[+39]
	ON11	5′-d(GG**X** A**X**A TAT AGG C)		-443	-300	-303	-387	-233	-232
10									
	ON2	3′-d(CCA TAT ATA TCC G)		[-24]	[+82]	[+100]	[-2]	[+92]	[+104]
	ON12	5′-d(GG**X** ATA **X**AT AGG C)		-401	-340	-308	-339	-266	-233
11									
	ON2	3′-d(CCA TAT ATA TCC G)		[+18]	[+42]	[+95]	[+46]	[+59]	[+103]
	ON13	5′-d(GG**X** ATA TA**X** AGG C)		-421	-399	-334	-361	-319	-257
12									
	ON2	3′-d(CCA TAT ATA TCC G)		[-2]	[-17]	[+69]	[+24]	[+6]	[+79]
	ON1	5′-d(GGT ATA TAT AGG C)		-413	-385	-373	-352	-306	-289
13									
	ON14	3′-d(CCA **X**A**X** ATA TCC G)		[+6]	[-3]	[+30]	[+33]	[+19]	[+47]
	ON1	5′-d(GGT ATA TAT AGG C)		-438	-414	-381	-371	-328	-293
14									
	ON15	3′-d(CCA **X**AT A**X**A TCC G)		[-19]	[-32]	[+22]	[+14]	[-3]	[+43]

	ON1	5'-d(GGT ATA TAT AGG C)	-401	-405	-395	-338	-322	-307
15								
	ON16	3'-d(CCA **X**AT ATA **X**CC G)	[+18]	[-23]	[-8]	[+47]	[+3]	[+29]

[a] The thermodynamic parameters were extracted as described in Table S2. The relative changes ($\Delta\Delta H$ and $\Delta(T^{293}\Delta S)$) are calculated relative to **ON1**:**ON2**; [b] Determined based upon single measurement.

Table S4. Hybridization data for Invader LNA at different ionic strengths.[a]

				T_m[Δ T_m] (ºC)			ΔG^{293} [$\Delta\Delta G^{293}$] (kJ/mol)		
Entry	ON	Duplex	**[Na^+] =**	10 mM	110 mM	710 mM	10 mM	110 mM	710 mM
1	**ON3**	5′-d(GG**X** ATA TAT AGG C)		nt	36.5	42.5	nd	-48	-51
	ON7	3′-d(CCA **X**AT ATA TCC G)			[-1.0]	[-3.0]		[+9]	[+17]
2	**ON4**	5′-d(GGT A**X**A TAT AGG C)		19.5	41.0	47.5	-35	-60	-58
	ON8	3′-d(CCA TA**X** ATA TCC G)		[+1.0]	[+3.5]	[+2.0]	[-1]	[-3]	[+10]
3	**ON5**	5′-d(GGT ATA **X**AT AGG C)		20.5	40.5	47.5	-36	-60	-61
	ON9	3′-d(CCA TAT A**X**A TCC G)		[+2.0]	[+3.0]	[+2.0]	[-2]	[-3]	[+7]
4	**ON6**	5′-d(GGT ATA TA**X** AGG C)		15.5	36.0	44.5	nd	-51	-55
	ON10	3′-d(CCA TAT ATA **X**CC G)		[-3.0]	[-1.5]	[-1.0]		[+6]	[+13]
5	**ON11**	5′-d(GG**X** A**X**A TAT AGG C)		24.5	48.0	59.0	-39	-55	-63
	ON14	3′-d(CCA **X**A**X** ATA TCC G)		[+6.0]	[+10.5]	[+13.5]	[-5]	[+2]	[+5]
6	**ON12**	5′-d(GG**X** ATA **X**AT AGG C)		31.0	53.0	61.5	-43	-56	-64
	ON15	3′-d(CCA **X**AT A**X**A TCC G)		[+12.5]	[+15.5]	[+16.0]	[-9]	[+1]	[+4]
7	**ON13**	5′-d(GG**X** ATA TA**X** AGG C)		24.0	48.0	56.0	-39	-55	-63
	ON16	3′-d(CCA **X**AT ATA **X**CC G)		[+5.5]	[+10.5]	[+10.5]	[-5]	[+2]	[+5]

[a] For conditions see Table S2. nt = no transition. nd = not determined. The "*interstrand zipper arrangement*" nomenclature is used herein to describe the relative arrangement between two **X** monomers positioned on opposing strands in a duplex. The number '*n*' describes the distance measured in number of base pairs and is positive if an **X** monomer is shifted toward the 5'-side of its own strand relative to a second reference **X** monomer on the other strand. Conversely, *n* is negative if an **X** monomer is shifted toward the 3'-side of its own strand relative to a second reference **X** monomer on the other strand. Hence, the two **X** monomers in 5'-d(GGT A**X**A TAT AGG C):3'-d(CCA TA**X** ATA TCC G) (**ON4**:**ON8**) are in an "+1 interstrand zipper arrangement", while in a "-1 zipper" in 5'-d(GGT A**X**A TAT AGG C):3'-d(CCA **X**AT ATA TCC G) (**ON4**:**ON7**).

Table S5. Entropy and enthalpy data for Invader LNA at different ionic strengths.[a]

				ΔH [$\Delta\Delta H$] (kJ/mol)			$(T^{293}\Delta S)$ [$\Delta(T^{293}\Delta S)$] (kJ/mol)		
	ON	Duplex	**[Na^+] =**	10 mM	110 mM	710 mM	10 mM	110 mM	710 mM
1	**ON3**	5'-d(GG**X** ATA TAT AGG C)		nd	-262	-214	nd	-214	-164
	ON7	3'-d(CCA **X**AT ATA TCC G)			[+120]	[+189]		[+111]	[+172]
2	**ON4**	5'-d(GGT A**X**A TAT AGG C)		-393	-360	-302	-359	-301	-245
	ON8	3'-d(CCA TA**X** ATA TCC G)		[+26]	[+22]	[+101]	[+26]	[+24]	[+91]
3	**ON5**	5'-d(GGT ATA **X**AT AGG C)		-345	-375	-303	-309	-315	-242
	ON9	3'-d(CCA TAT A**X**A TCC G)		[+74]	[+7]	[+100]	[+76]	[+10]	[+94]
4	**ON6**	5'-d(GGT ATA TA**X** AGG C)		nd	-311	-254	nd	-260	-200
	ON10	3'-d(CCA TAT ATA **X**CC G)			[+71]	[+149]		[+65]	[+136]
5	**ON11**	5'-d(GG**X** A**X**A TAT AGG C)		-234	-219	-238	-195	-165	-175
	ON14	3'-d(CCA **X**A**X** ATA TCC G)		[+185]	[+163]	[+165]	[+190]	[+160]	[+161]
6	**ON12**	5'-d(GG**X** ATA **X**AT AGG C)		-202	-209	-233	-159	-152	-169
	ON15	3'-d(CCA **X**AT A**X**A TCC G)		[+217]	[+173]	[+170]	[+226]	[+173]	[+167]
7	**ON13**	5'-d(GG**X** ATA TA**X** AGG C)		-237	-230	-250	-198	-175	-187
	ON16	3'-d(CCA **X**AT ATA **X**CC G)		[+182]	[+152]	[+153]	[+187]	[+150]	[+149]

[a] The thermodynamic parameters were extracted as described in Table S2. The relative changes ($\Delta\Delta H$ and $\Delta(T^{293}\Delta S)$) are calculated relative to **ON1**:**ON2.**

Table S6. Calculated free energy, ΔG^{293}_{rec}, for recognition of dsDNA target **ON1**:**ON2** by Invader LNA probes at 293 K and different ionic strengths.

Entry	ON	Duplex	[Na^+] =	ΔG^{293a}_{rec} (kJ/mol) 10 mM	110 mM	710 mM
1	**ON3** **ON7**	5′-d(GG**X** ATA TAT AGG C) 3′-d(CCA **X**AT ATA TCC G)		nd	-26	-26
2	**ON4** **ON8**	5′-d(GGT A**X**A TAT AGG C) 3′-d(CCA TA**X** ATA TCC G)		-23	-19	-29
3	**ON5** **ON9**	5′-d(GGT ATA **X**AT AGG C) 3′-d(CCA TAT A**X**A TCC G)		-26	-22	-23
4	**ON6** **ON10**	5′-d(GGT ATA TA**X** AGG C) 3′-d(CCA TAT ATA **X**CC G)		nd	-24	-25
5	**ON11** **ON14**	5′-d(GG**X** A**X**A TAT AGG C) 3′-d(CCA **X**A**X** ATA TCC G)		-45	-34	-24
6	**ON12** **ON15**	5′-d(GG**X** ATA **X**AT AGG C) 3′-d(CCA **X**AT A**X**A TCC G)		-53	-47	-31
7	**ON13** **ON16**	5′-d(GG**X** ATA TA**X** AGG C) 3′-d(CCA **X**AT ATA **X**CC G)		-51	-50	-35

[a] ΔG^{293}_{rec} = ΔG^{293} (probe strand 1 : target strand 1) + ΔG^{293} (probe strand 2 : target strand 2) - ΔG^{293} (dsDNA target) - ΔG^{293} (Invader LNA). As a representative example, the thermodynamic driving force for recognition of dsDNA target **ON1**:**ON2** by Invader LNA **ON4**:**ON8** at medium salt concentration is calculated as: ΔG^{293}_{rec}(**ON4**:**ON8**+**ON1**:**ON2**) = ΔG^{293} (**ON4**:**ON2**) + ΔG^{293} (**ON1**:**ON8**) – ΔG^{293} (**ON1**:**ON2**) - ΔG^{293} (**ON4**:**ON8**) = -65.8 kJ/mol + (-69.5 kJ/mol) - (-56.9 kJ/mol) - (-59.6 kJ/mol) = -18.8 kJ/mol.

Additional discussion of thermodynamic parameters.

As expected, the stability of reference duplexes **ON1**:**ON2** increases with higher salt concentration due to increased electrostatic screening of the negative charges from the backbones (entry 1, Table S2). The relative stability of duplexes between singly or doubly modified 2'-*N*-(pyren-1-yl)methyl-2'-amino-α-L-LNA and complementary DNA generally increased with decreasing ionic strengths (compare ΔT_m and $\Delta\Delta G^{293}$ at different [Na^+], entries 2-15, Table S2). The increased thermal affinity toward DNA targets is, mostly and irrespectively of ionic strength, the result of less unfavorable entropic contributions, which are not fully counterbalanced by less favorable enthalpic contributions (compare $\Delta\Delta H$ and $\Delta(T^{293}\Delta S)$, entries 2-15, Table S3). As previously discussed (S1,S2), this reflects the ability of the preorganized 2'-amino-α-L-LNA building blocks to direct appended intercalators to the duplex core. Oddly, a non-linear trend was generally observed for $\Delta\Delta H$ and $\Delta(T^{293}\Delta S)$ as a function of ionic strength, e.g., enthalpic and entropic contributions were found to be most and least favorable in medium salt buffers, respectively (Table S3). Accordingly, the underlying reasons for the trends in $\Delta\Delta G^{293}$ are not immediately apparent from the corresponding $\Delta\Delta H$ and $\Delta(T^{293}\Delta S)$ values (Table S3).

Single hotspot Invader LNA probes do not display a clear correlation between ΔT_m-values and ionic strength, whereas $\Delta\Delta G^{293}$ values suggest a weak relative destabilization with increasing ionic strengths (compare ΔT_m and $\Delta\Delta G^{293}$ at different [Na^+], entries 1-4, Table S4). Hybridization data of double hotspot Invader LNA probes exhibit opposing trends, i.e., $\Delta\Delta G^{293}$ values increase (i.e., less stable) with increasing ionic strength, while smaller ΔT_m-values (i.e., less stable) are observed with lower ionic strengths (entries 5-7, Table S4). As discussed in the main manuscript, this is a reflection of the substantial entropic contributions to hybridization observed for Invader LNA probes rendering $\Delta\Delta G$-values highly temperature dependent (Table S5). There is no clear correlation between $\Delta\Delta H$ or $\Delta(T^{293}\Delta S)$ values and ionic strength for single hotspot Invader LNA probes (entries 1-4, Table S5). In contrast, entropic contributions are more

favorable with decreasing ionic strengths for double hotspot Invader LNA probes (and vice versa for enthalpic contributions, entries 5-7, Table S5)

Accordingly, the ionic strength of the hybridization buffer influences the available free energy, ΔG_{rec}^{293}, for recognition of dsDNA targets. Approximately 20-25 kJ/mol of free energy is available for recognition of dsDNA target **ON1**:**ON2** by all single hotspot Invader LNA probes irrespective of the ionic strength (entries 1-4, Table S6). In contrast, significantly more free energy is available at lower ionic strengths for targeting of dsDNA targets by double hotspot Invader LNA probes (entries 5-7, Table S6). In conclusion, Invader LNA probes have pronounced dsDNA affinity in a variety of buffers, including those mimicking physiological conditions.

Table S7. Hybridization data for **ON3**-**ON16** vs complementary RNA in medium salt buffer.[a]

ON	ON sequence	T_m (ºC)	ΔT_m (ºC)
ON1	5′-d(GGT ATA TAT AGG C) 3′-r(CCA UAU AUA UCC G)	37.0	-
ON2	5′-r(GGU AUA UAU AGG C) 3′-d(CCA TAT ATA TCC G)	39.5	-
ON3	5′-d(GG**X** ATA TAT AGG C) 3′-r(CCA UAU AUA UCC G)	37.5	+0.5
ON4	5′-d(GGT A**X**A TAT AGG C) 3′-r(CCA UAU AUA UCC G)	41.5	+4.5
ON5	5′-d(GGT ATA **X**AT AGG C) 3′-r(CCA UAU AUA UCC G)	41.0	+4.0
ON6	5′-d(GGT ATA TA**X** AGG C) 3′-r(CCA UAU AUA UCC G)	40.0	+3.0
ON7	5′-r(GGU AUA UAU AGG C) 3′-d(CCA **X**AT ATA TCC G)	42.5	+3.0
ON8	5′-r(GGU AUA UAU AGG C) 3′-d(CCA TA**X** ATA TCC G)	45.0	+5.5
ON9	5′-r(GGU AUA UAU AGG C) 3′-d(CCA TAT A**X**A TCC G)	44.5	+5.0
ON10	5′-r(GGU AUA UAU AGG C) 3′-d(CCA TAT ATA **X**CC G)	45.5	+6.0
ON11	5′-d(GG**X** A**X**A TAT AGG C) 3′-r(CCA UAU AUA UCC G)	44.0	+6.0
ON12	5′-d(GG**X** ATA **X**AT AGG C) 3′-r(CCA UAU AUA UCC G)	48.0	+11.0
ON13	5′-d(GG**X** ATA TA**X** AGG C) 3′-r(CCA UAU AUA UCC G)	44.5	+7.5
ON14	5′-r(GGU AUA UAU AGG C) 3′-d(CCA **X**A**X** ATA TCC G)	49.0	+12.0
ON15	5′-r(GGU AUA UAU AGG C) 3′-d(CCA **X**AT A**X**A TCC G)	48.5	+11.5
ON16	5′-r(GGU AUA UAU AGG C) 3′-d(CCA **X**AT ATA **X**CC G)	49.5	+12.5

[a] T_m-values were determined as the maximum of the first derivative of the melting curve (A_{260} vs T) recorded in medium salt buffer ($[Na^+]$ = 110 mM, $[Cl^-]$ = 100 mM, pH 7.0 (adjusted with NaH_2PO_4/Na_2HPO_4)), using 1.0 uM of each strands. ΔT_m-values calculated relative to reference duplexes (**ON1**:**RNA** and **RNA**:**ON2**).

Table S8. Hybridization data for duplexes with selected interstrand zipper arrangements of **X** monomers.[a]

	Zipper arrangement	Duplex	T_m (ºC)	ΔT_m (ºC)
ON1	-	5′- d(GGT ATA TAT AGG C)	37.5	-
ON2		3′- d(CCA TAT ATA TCC G)		
ON6	-3	5′- d(GGT ATA TA**X** AGG C)	59.0	+21.5
ON8		3′- d(CCA TA**X** ATA TCC G)		
ON5	-1	5′- d(GGT ATA **X**AT AGG C)	55.5	+18.0
ON8		3′- d(CCA TA**X** ATA TCC G)		
ON6	-1	5′- d(GGT ATA TA**X** AGG C)	53.5	+16.0
ON9		3′- d(CCA TAT A**X**A TCC G)		
ON3	+1	5′- d(GG**X** ATA TAT AGG C)	36.5	**-1.0**
ON7		3′- d(CCA **X**AT ATA TCC G)		
ON4	+1	5′- d(GGT A**X**A TAT AGG C)	41.0	**+3.5**
ON8		3′- d(CCA TA**X** ATA TCC G)		
ON5	+1	5′- d(GGT ATA **X**AT AGG C)	40.5	**+3.0**
ON9		3′- d(CCA TAT A**X**A TCC G)		
ON6	+1	5′- d(GGT ATA TA**X** AGG C)	36.0	**-1.5**
ON10		3′- d(CCA TAT ATA **X**CC G)		
ON4	+3	5′- d(GGT A**X**A TAT AGG C)	58.0	+20.5
ON9		3′- d(CCA TAT A**X**A TCC G)		
ON5	+3	5′- d(GGT ATA **X**AT AGG C)	58.5	+21.0
ON10		3′- d(CCA TAT ATA **X**CC G)		
ON4	+5	5′- d(GGT A**X**A TAT AGG C)	59.0	+21.5
ON10		3′- d(CCA TAT ATA **X**CC G)		

[a] For conditions see Table S2. ΔT_m-values calculated relative to **ON1**:**ON2** reference duplex

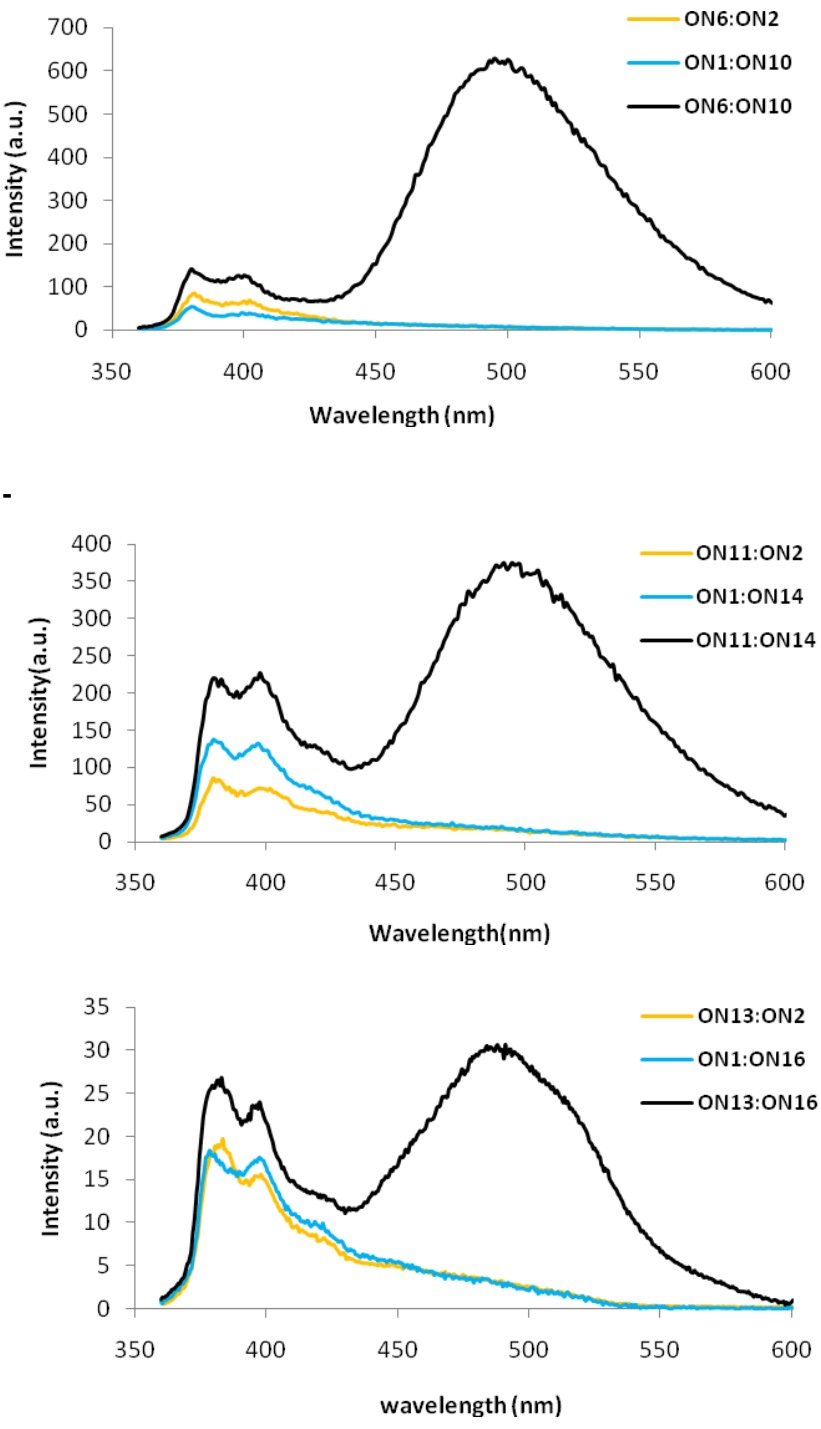

Figure S2. Steady-state fluorescence emission spectra of Invader LNA probes **ON6**:**ON10**, **ON11**:**ON14** and **ON13**:**ON16**, and the corresponding probe:target duplexes. Conditions: each strand at 1.0 μM concentration, [Na^+] = 110 mM, pH 7.0, 20 ºC, λ_{ex} = 340 nm (bottom) or 335 nm (upper and middle). Notice different scales are used for the y-axes.

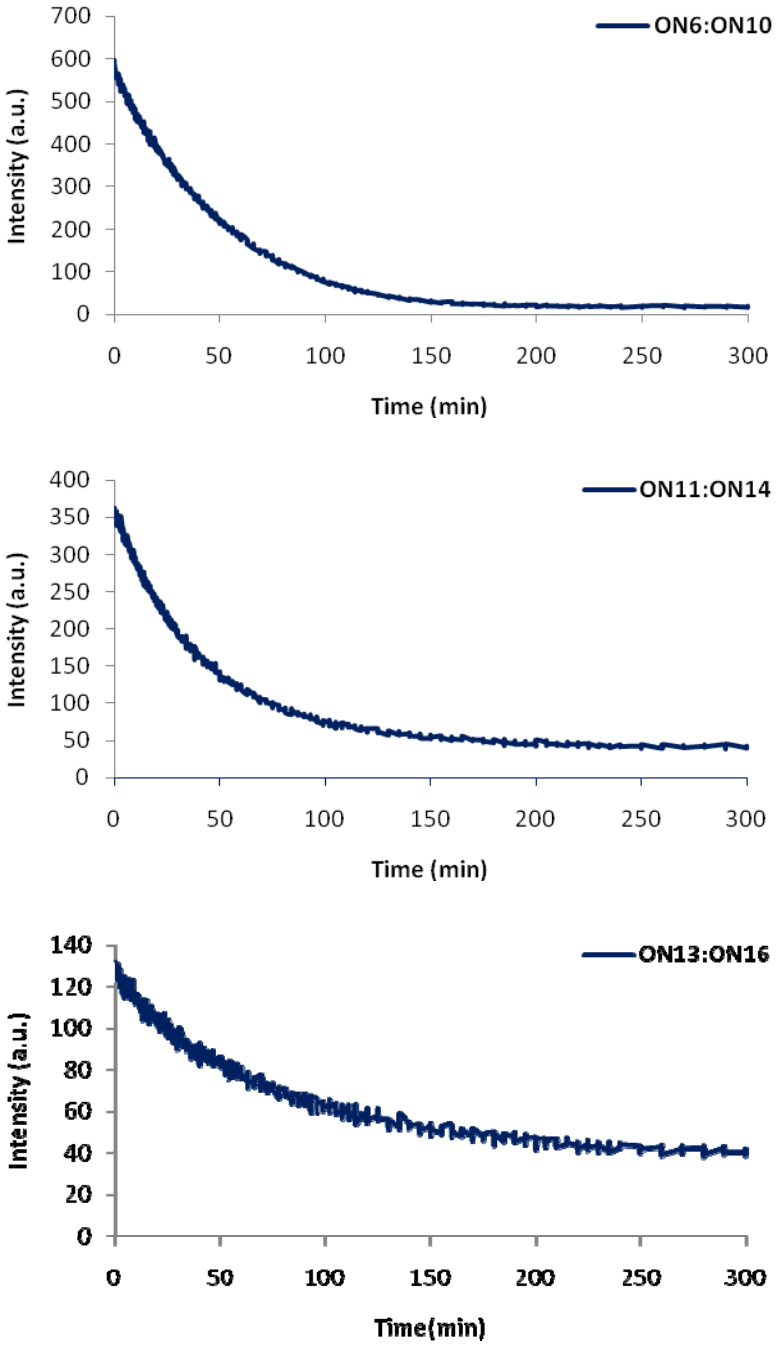

Figure S3. Fluorescence signal decay profiles at λ_{em} = 495 nm as a function of time upon addition of equimolar quantities of pre-annealed Invader LNA probes **ON6**:**ON10**, **ON11**:**ON14** or **ON13**:**ON16** to pre-annealed isosequential dsDNA target **ON1:ON2** (upper, middle and lower panel, respectively). Conditions are as described in Figure 3. Note that different y-axes are used.

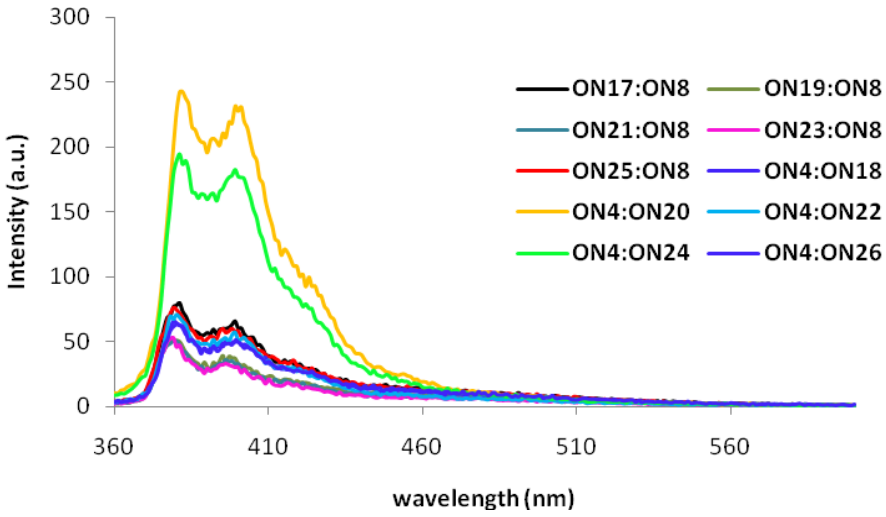

Figure S4. Steady-state fluorescence emission spectra of duplexes between **ON4** or **ON8** and mismatched DNA targets. Sequences of **ON17**-**ON26** are shown in Table S9. Conditions: each strand at 1.0 μM concentration, $[Na^+]$ = 110 mM, pH 7.0, 20 ºC, λ_{ex} = 335 nm.

Additional discussion regarding recognition of mismatched dsDNA targets by Invader LNA probe ON4:ON8.

Duplexes between 2'-*N*-(pyren-1-yl)methyl-2'-amino-α-L-LNA and mismatched DNA targets only exhibit negligible signals at 495 nm (Fig. S4). Complete recognition of non-isosequential dsDNA targets by Invader LNA probe **ON4**:**ON8** would therefore have resulted in complete disappearance of signal at λ_{em} = 495 nm (e.g., sum of **ON17**:**ON8** and **ON4**:**ON18**), and it can therefore be concluded that Invader LNA probes exhibit good discrimination of non-isosequential dsDNA targets.

Table S9. Hybridization data for duplexes between **ON1** or **ON2** and mismatched DNA targets.[a]

Entry	ON	Sequence	T_m [ΔT_m]
1	**ON17**	5'- d(GGA ATA TAT AGG C)	27.0
	ON2	3'- d(CCA TAT ATA TCC G)	(-10.5)
2	**ON19**	5'- d(GGT ATC TAT AGG C)	25.5
	ON2	3'- d(CCA TAT ATA TCC G)	(-12.0)
3	**ON21**	5'- d(GGT ATG TAT AGG C)	31.0
	ON2	3'- d(CCA TAT ATA TCC G)	(-6.5)
4	**ON23**	5'- d(GGT ATT TAT AGG C)	27.0
	ON2	3'- d(CCA TAT ATA TCC G)	(-10.5)
5	**ON25**	5'- d(GGT ATA TAA AGG C)	24.0
	ON2	3'- d(CCA TAT ATA TCC G)	(-13.5)
6	**ON1**	5'- d(GGT ATA TAT AGG C)	26.5
	ON18	3'- d(CCT TAT ATA TCC G)	(-12.0)
7	**ON1**	5'- d(GGT ATA TAT AGG C)	30.0
	ON20	3'- d(CCA TAG ATA TCC G)	(-7.5)
8	**ON1**	5'- d(GGT ATA TAT AGG C)	26.0
	ON22	3'- d(CCA TAC ATA TCC G)	(-11.5)
9	**ON1**	5'- d(GGT ATA TAT AGG C)	24.5
	ON24	3'- d(CCA TAA ATA TCC G)	(-13.0)
10	**ON1**	5'- d(GGT ATA TAT AGG C)	27.5
	ON26	3'- d(CCA TAT ATT TCC G)	(-10.0)

[a] Conditions as specified in Table S2. Underlined positions highlight position of mismatched base pairs. ΔT_m = change in T_m value relative to fully matched **ON1**:**ON2**.

REFERENCES

S1) T. S. Kumar, A. S. Madsen, M. E. Østergaard, S. P. Sau, J. Wengel and P. J. Hrdlicka, J. Org. Chem., 2009, **74**, 1070-1081.

S2) T. S. Kumar, A. S. Madsen, M. E. Østergaard, J. Wengel and P. J. Hrdlicka, *J. Org. Chem.*, 2008, **73**, 4188-4201.